Article

Intercalation Is Not Required for DNA Light-Switch Behavior

Daniel A. Lutterman, Abdellatif Chouai, Yao Liu, Yujie Sun,
Cristina D. Stewart, Kim R. Dunbar, and Claudia Turro

J. Am. Chem. Soc., **2008**, 130 (4), 1163-1170 • DOI: 10.1021/ja071001v

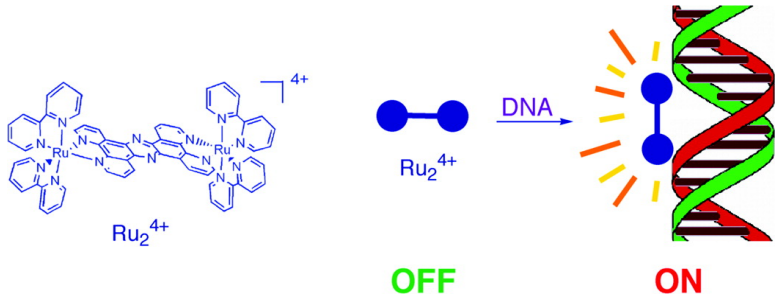

More About This Article

Additional resources and features associated with this article are available within the HTML version:

- Supporting Information
- Links to the 1 articles that cite this article, as of the time of this article download
- Access to high resolution figures
- Links to articles and content related to this article
- Copyright permission to reproduce figures and/or text from this article

View the Full Text HTML

J|A|C|S
ARTICLES
Published on Web 01/08/2008

Intercalation Is Not Required for DNA Light-Switch Behavior

Daniel A. Lutterman,[†] Abdellatif Chouai,[‡] Yao Liu,[†] Yujie Sun,[†] Cristina D. Stewart,[†] Kim R. Dunbar,*[,‡] and Claudia Turro*[,†]

Department of Chemistry, The Ohio State University, Columbus, Ohio 43210, and Department of Chemistry, Texas A&M University, College Station, Texas 77843

Received February 12, 2007; E-mail: turro@chemistry.ohio-state.edu; dunbar@mail.chem.tamu.edu

Abstract: The DNA light-switch complex $[Ru(bpy)_2(tpphz)]^{2+}$ (**1**, bpy = 2,2′-bipyridine, tpphz = tetrapyrido-[3,2-*a*:2′,3′-*c*:3″,2″-*h*:2‴,3‴-*j*]phenazine) is luminescent when bound to DNA and in organic solvents and weakly emissive in water. To date, light-switch behavior by transition metal complexes has generally been regarded as confirmation of DNA intercalation. In contrast, the present work demonstrates that the nonintercalating bimetallic complex $[(bpy)_2Ru(tpphz)Ru(bpy)_2]^{4+}$ (**2**) behaves as a DNA light-switch. Weak emission from the ^{3}MLCT excited state of **2** is observed in water with $\lambda_{em} = 623$ nm ($\Phi_{em} = 1.4 \times 10^{-4}$), and a red shift ($\lambda_{em} = 702$ nm) and 40-fold increase in intensity are observed upon addition of 100 μM calf thymus DNA (ct-DNA). Addition of increasing concentrations of **2** to 1 mM herring sperm DNA does not result in an increase in the viscosity of the solution, indicating that the complex is not an intercalator. Additionally, experiments were conducted to ensure that the emission enhancement did not arise from threading intercalation of the complex. The in situ generation of **2** intercalated between the base pairs of ct-DNA in a threading fashion, however, exhibits emission maximum at 685 nm, which is blue-shifted from that of surface-bound **2**. DFT calculations show low-lying orbitals in **2** that are expected to exhibit nonemissive character when contributing to the MLCT state, in accord with the lower emission intensity observed for **2** relative to that for **1**. To our knowledge, the present work is the first example of a nonintercalating light-switch metal complex, thus showing that light-switch behavior cannot be used exclusively as confirmation of intercalation.

Introduction

Since the discovery that the DNA intercalation of $[Ru(bpy)_2(dppz)]^{2+}$ (bpy = 2,2′-bipyridine, dppz = dipyrido[3,2-*a*:2′,3′-*c*]phenazine) results in enhanced emission (structure shown in Figure 1a),[1,2] numerous "DNA light-switch" compounds have been discovered.[3−9] One such complex, $[Ru(bpy)_2(tpphz)]^{2+}$ (**1**; tpphz = tetrapyrido[3,2-*a*:2′,3′-*c*:3″,2″-*h*:2‴,3‴-*j*]-phenazine), was also recently reported to behave as a DNA light-switch (Figure 1a).[10] These systems are of interest because they may have potential applications in sensing and signaling, as well as in data storage and communication.[1,2,11−14] To date, light-switch behavior by transition metal complexes has only been reported for intercalators and has generally been regarded as confirmation of DNA intercalation.[15−19]

The factors that govern the luminescence enhancement of $[Ru(bpy)_2(dppz)]^{2+}$ in organic solvents and in the presence of DNA relative to water are now relatively well understood. The emission from $[Ru(bpy)_2(dppz)]^{2+}$ arises from a Ru → dppz metal-to-ligand charge transfer (^{3}MLCT) excited state (λ_{em} = 620 nm, $\tau_{em} = 970$ ns in butyronitrile, 293 K).[20,21] The emission lifetime of $[Ru(bpy)_2(dppz)]^{2+}$ decreases with increasing temperature in the range 254−350 K, which is attributed to the thermal population of nonemissive ^{3}dd state(s) as is the case for $[Ru(bpy)_3]^{2+}$.[20,21] Unlike $[Ru(bpy)_3]^{2+}$, however, cooling of $[Ru(bpy)_2(dppz)]^{2+}$ below 254 K also results in a decrease in lifetime.[20,21] This temperature dependence of the luminescence is believed to arise from the presence of a lowest-energy nonemissive excited dark state (D), a close thermally accessible emissive bright state (B), and nonemissive ^{3}dd state(s) at significantly higher energy, as schematically depicted in Figure 1b.[20,21]

[†] The Ohio State University.
[‡] Texas A&M University.

(1) Friedman, A. E.; Chambron, J. C.; Sauvage, J. P.; Turro, N. J.; Barton, J. K. *J. Am. Chem. Soc.* **1990**, *112*, 4960.
(2) Hartshorn, R. M.; Barton, J. K. *J. Am. Chem. Soc.* **1992**, *114*, 5919.
(3) Holmlin, R. E.; Barton, J. K. *Inorg. Chem.* **1995**, *34*, 7.
(4) Holmlin, R. E.; Tong, R. T.; Barton, J. K. *J. Am. Chem. Soc.* **1998**, *120*, 9724.
(5) Moucheron, C.; Kirsch-De Mesmaeker, A.; Choua, S. *Inorg. Chem.* **1997**, *36*, 584.
(6) Arounaguiri, S.; Maiya, B. G. *Inorg. Chem.* **1999**, *38*, 842.
(7) Zhang, Q.-L.; Liu, J.-H.; Ren, X.-Z.; Xu, H.; Huang, Y.; Liu, J.-Z.; Ji, L.-N. *J. Inorg. Biochem.* **2003**, *95*, 194.
(8) Nair, R. B.; Murphy, C. J. *J. Inorg. Biochem.* **1998**, *69*, 129.
(9) Tuite, E.; Lincoln, P.; Norden, B. *J. Am. Chem. Soc.* **1997**, *119*, 239.
(10) Liu, Y.; Chouai, A.; Degtyareva, N. N.; Lutterman, D. A.; Dunbar, K. R.; Turro, C. *J. Am. Chem. Soc.* **2005**, *127*, 10796.
(11) Ling, L.-S.; He, Z.-H.; Song, G.-W.; Zeng, Y. E.; Wang, C.; Bai, C.-L.; Chen, X.-D.; Shen, P. *Anal. Chim. Acta* **2001**, *436*, 207.
(12) Ling, L.-S.; He, Z.-K.; Chen, F.; Zeng, Y.-E. *Talanta* **2003**, *59*, 269.
(13) de Silva, A. P.; McClenaghan, N. D. *Chem.−Eur. J.* **2004**, *10*, 574.
(14) Jiang, Y.; Fang, X.; Bai, C. *Anal. Chem.* **2004**, *76*, 5230.
(15) Erkkila, K. E.; Odom, D. T.; Barton, J. K. *Chem. Rev.* **1999**, *99*, 2777.
(16) Holmlin, R. E.; Yao, J. A.; Barton, J. K. *Inorg. Chem.* **1999**, *38*, 174.
(17) Delaney, S.; Pascaly, M.; Bhattacharya, P. K.; Han, K.; Barton, J. K. *Inorg. Chem.* **2002**, *41*, 1966.
(18) Mariappan, M.; Maiya, B. G. *Eur. J. Inorg. Chem.* **2005**, 2164.
(19) Ji, L.-N.; Zou, X.-H.; Liu, J.-G. *Coord. Chem. Rev.* **2001**, *216*, 513.
(20) Brennaman, M. K.; Alstrum-Acevedo, J. H.; Fleming, C. N.; Jang, P.; Meyer, T. J.; Papanikolas, J. M. *J. Am. Chem. Soc.* **2002**, *124*, 15094.
(21) Brennaman, M. K.; Meyer, T. J.; Papanikolas, J. M. *J. Phys. Chem. A* **2004**, *108*, 9938.

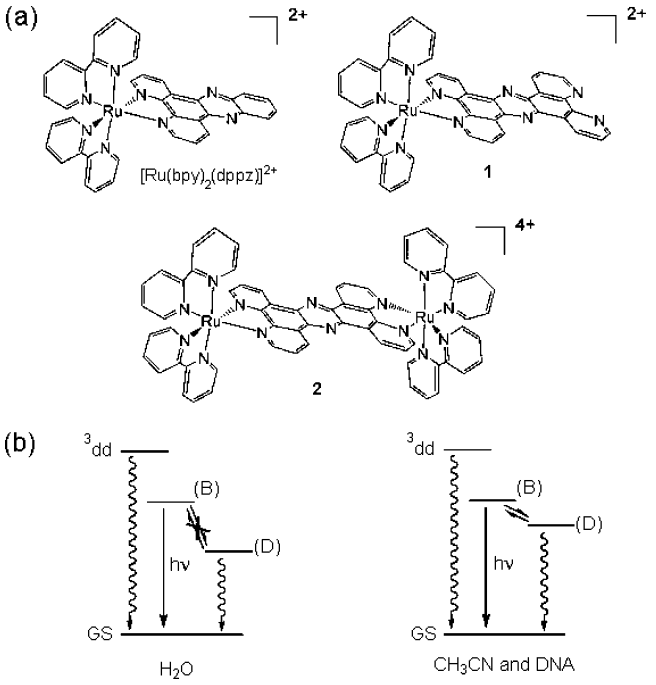

Figure 1. (a) Molecular structures of $[Ru(bpy)_2(dppz)]^{2+}$, $[Ru(bpy)_2(tpphz)]^{2+}$ (**1**), and $[(bpy)_2Ru(tpphz)Ru(bpy)_2]^{4+}$ (**2**). (b) Energy level diagrams of $[Ru(bpy)_2(dppz)]^{2+}$ and **1** in H_2O (left) and CH_3CN and DNA (right), where the labels B and D refer to emissive and nonemissive ^{3}MLCT excited states (see text).

It has been proposed that the lowest-energy dark state, D, in $[Ru(bpy)_2(dppz)]^{2+}$ arises from a ^{3}MLCT transition from the Ru(II) to the phenazine part of the dppz ligand, while the bright state, B, is a result of charge transfer from the metal center to the bpy portion of the same ligand.[20−22] In general, it is believed that the energy of the dark state varies with the polarity of the solvent, such that the relative energies of these emissive and nonemissive excited states dictate the intensity and lifetime of the luminescence at a given temperature. In water or buffer, the energy separation between these two states is too large for thermal population of the emissive state at 298 K, making the complex nonemissive in this solvent (Figure 1b).[20,21] Intercalation of the dppz ligand between the DNA bases results in an increase in energy of the dark ^{3}MLCT state, thus making the emissive state thermally accessible and turning on the emission (Figure 1b).[20,21]

Complex **1** binds to DNA through the intercalation of the tpphz ligand between the bases of the duplex, resulting in an increase in the luminescence intensity of **1**, thus making it a "DNA light-switch".[10] Owing to the presence of an open bidentate coordination site in **1** (Figure 1a), transition metals are able to bind to the complex, thus forming tpphz-bridged bimetallic systems. The enhanced emission of DNA intercalated **1** was recently shown to be "turned off" by the coordination of various transition metals to the distal nitrogen atoms of the tpphz ligand through the formation of nonemissive ground-state adducts of the type $[(bpy)_2Ru-tpphz-M]^{4+}$ (**1**−$\mathbf{M^{2+}}$; M^{2+} = Ni^{2+}, Zn^{2+}, Co^{2+}).[10] Although in the **1**−$\mathbf{Co^{2+}}$ and **1**−$\mathbf{Ni^{2+}}$ systems the decrease in luminescence may be partially ascribed to energy or electron transfer, such quenching is not possible in **1**−$\mathbf{Zn^{2+}}$. In the **1**−$\mathbf{M^{2+}}$ systems, the changes in the electronic structure that take place upon coordination of M^{2+} to the tpphz ligand of **1** are believed to generally result in lower emission intensity.[10]

It was recently reported that the bimetallic complex $[(bpy)_2Ru(tpphz)Ru(bpy)_2]^{4+}$ (**2**, Figure 1a) intercalates between the DNA bases in a threading fashion, thus resulting in emission enhancement.[23] Various techniques used in the present work, however, show that **2** does not intercalate when the sample is extensively purified. Although **2** does not intercalate between the DNA bases, this work also demonstrates that the complex behaves as a DNA light-switch. In addition, when the intercalation of **2** is accomplished by the photochemical generation of a *cis*-$[Ru(bpy)_2]^{2+}$ fragment, which then coordinates to the distal nitrogen atoms of the tpphz ligand of a sample of **1** intercalated between the bases of DNA, the emission maximum is different from those of the free complex in buffer and that which is electrostatically bound to DNA. To our knowledge, these results represent the first example of a nonintercalating light-switch complex and the photoinduced generation of a threaded intercalator.

Experimental Section

Materials. $[Ru(bpy)_2(tpphz)](PF_6)_2$ was prepared by published methods.[24,25] $[Ru(bpy)_2(tpphz)]Cl_2$ (**1**) was precipitated by the addition of a saturated Bu_4NCl acetone solution to $[Ru(bpy)_2(tpphz)](PF_6)_2$ in acetone. The orange solid was filtered, washed with acetone and diethyl ether, and dried under vacuum. $[(bpy)_2Ru(tpphz)Ru(bpy)_2](PF_6)_4$ was prepared by a literature procedure,[24] and $[(bpy)_2Ru(tpphz)Ru(bpy)_2]Cl_4$ (**2**) was precipitated in a similar fashion as described for **1**. Complex **2** was initially purified through column chromatography using a silica gel and Sephadex G-15 columns, followed by reverse-phase HPLC (Supporting Information). ^{1}H NMR (500 MHz) in CD_3CN-d_3 δ (splitting, integration): 7.27 (t, 4H), 7.50 (t, 4H), 7.77 (d, 4H), 7.88 (d, 4H), 8.02 (m, 8H), 8.15 (t, 4H), 8.30 (d, 4H), 8.59 (d, 4H), 8.62 (d, 4H), 9.96 (d, 4H).

Instrumentation. Electronic absorption measurements were performed on a Hewlett-Packard diode array spectrophotometer (HP 8453) with HP 8453 Win System software. A 150 W Xe lamp housed in a Milliarc compact arc lamp housing and powered by a PTI model LPS-220 power supply was used in the steady-state photolysis experiments; the wavelength of the light reaching the sample was controlled with colored glass long-pass filters (CVI).

^{1}H NMR spectra were recorded on a Bruker DRX-500 spectrometer. The electrochemistry measurements were performed on a Cypress Systems CS-1200 instrument with a single-compartment three-electrode cell. The working electrode was a 1.0-mm-diameter Pt disk (Cypress or Bass) with a Pt wire auxiliary electrode and a Ag/Ag^+ pseudoreference electrode. A Helwlett-Packard HP 1100 series HPLC was used in the separations.

Methods. Complex **2** was purified by reverse-phase HPLC using a semi-prep Vydac C18 column and eluted with a mixture of 38% CH_3CN and 62% triethanolamine acetate (20 mM) buffer (pH = 7) at a flow rate of 5 mL/min. The elution of the complexes was monitored by their absorption using a diode array detector and takes place at 5.5 min for **1** and 3.1 min for **2**. Representative traces for the elution of **1** and **2** monitored at 450 and 442 nm, respectively, are shown in the Supporting Information (Figure S7). Following an injection containing a sample of **2**, the purified complex was collected from 2.6−4.9 min,

(22) Pourtois, G.; Beljonne, D.; Moucheron, C.; Schumm, S.; Mesmaeker, A. K.-D.; Lazzaroni, R.; Bredas, J.-L. *J. Am. Chem. Soc.* **2004**, *126*, 683.
(23) Rajput, C.; Rutkaite, R.; Swanson, L.; Haq, I.; Thomas, J. A. *Chem.−Eur. J.* **2006**, *12*, 4611.
(24) Bolger, J.; Gourdon, A.; Ishow, E.; Launay, J. *Inorg. Chem.* **1996**, *35*, 2937.
(25) Ishow, E.; Gourdon, A.; Launay, J.; Lecante, P.; Verelst, M.; Chiorboli, C.; Scandola, F.; Bignozzi, C. *Inorg. Chem.* **1998**, *37*, 3603.

a time window where complex **1** does not elute under these experimental conditions.

For the experiments where **2** was produced photochemically from **1** and $[Ru(bpy)_2(CH_3CN)_2]Cl_2$, the solvent mixture was ramped from 25 to 38% CH_3CN from 0 to 4 min, and was then held constant at 38% CH_3CN for 60 min. Under these conditions **1** and **2** elute at 7.7 and 6.0 min, respectively, while $[Ru(bpy)_2(CH_3CN)_2]Cl_2$ elutes at 3.2 min. Representative overlaid traces monitored at 450, 442, and 425 nm for **1**, **2**, and $[Ru(bpy)_2(CH_3CN)_2]Cl_2$, respectively, are shown in the Supporting Information (Figure S7). Complex **2** was generated photochemically from a sample of 100 μM **1** and 500 μM $[Ru(bpy)_2(CH_3CN)_2]Cl_2$ in H_2O was irradiated for 2 h ($\lambda_{irr} \geq 395$ nm). The sample was passed through a Sephadex column to remove the large excess of $[Ru(bpy)_2(CH_3CN)_2]Cl_2$ and$[Ru(bpy)_2(H_2O)_2]Cl_2$ produced from photolysis. The last fraction to elute from the Sephadex column was collected and concentrated. The sample was then injected into the HPLC, and eluent was collected between 4.8 and 7.0 min to ensure that no **1** or $[Ru(bpy)_2(CH_3CN)_2]Cl_2$ remained in the sample. The photophysical properties of the sample confirmed that **2** was the photoproduct of the experiment.

Deoxygenation for the luminescence experiments was performed by bubbling the sample with argon for ~15 min and keeping it under positive argon pressure during the experiment. Emission quantum yields were calculated using $[Ru(bpy)_3]^{2+}$ in CH_3CN ($\Phi_{ref} = 0.062$) as the reference actinometer (eq 1)[26]

$$\Phi_{em} = \Phi_{ref}\left(\frac{A_{ref}}{A_{em}}\right)\left(\frac{I_{em}}{I_{ref}}\right)\left(\frac{\eta_{em}}{\eta_{ref}}\right)^2 \quad (1)$$

where Φ_{em} and Φ_{ref} are the emission quantum yields of the sample and the reference, respectively, A_{ref} and A_{em} are the measured absorbance of the reference and sample at the excitation wavelength, respectively, I_{ref} and I_{em} are the integrated emission intensities of the reference and sample, respectively, and η_{ref} and η_{em} are the refractive index of the solvent of the reference and sample, respectively.[27] For the electrochemistry experiments, the samples were dissolved in dry acetonitrile (~10 mM) with 0.1 M $^tBu_4NPF_6$ as the electrolyte, and all potentials were determined by reference to the ferrocene/ferrocenium couple.[28] The DNA binding constant, K_b, was determined using equilibrium dialysis and from the changes in the absorption and emission intensities of the complex as a function of calf thymus DNA (ct-DNA) concentration as described previously.[10,16,29−33]

The molecular and electronic structure determinations on **1** and **2** were performed with density functional theory (DFT) using the Gaussian03 (G03) program package.[34] The B3LYP[35−37] functional together with the 6-31G* basis set were used for H, C, N, and O,[38] along with the Stuttgart/Dresden energy-consistent pseudopotentials for Ru.[39,40] All geometry optimizations were performed in C_1 symmetry with subsequent frequency analysis to ensure that the structures are local minima on the potential energy surface. The inclusion of solvent effects has recently been shown to be crucial when describing the electronic structure and absorption spectra of polypyridyl ruthenium complexes.[41,42] In the present work, solvent effects were modeled by single-point calculations based on the gas-phase optimized structures using the polarizable continuum model.[43−47] The orbital analysis was completed with Molekel 4.3.win32.[48] The vertical singlet transition energies of the complexes were computed at the time-dependent density functional theory (TDDFT) level in H_2O and CH_3CN within G03 by using the optimized structure for the ground state.

Results and Discussion

Synthesis, Characterization, and Purification of $[(bpy)_2Ru(tpphz)Ru(bpy)_2]Cl_4$ (2). $[(bpy)_2Ru(tpphz)Ru(bpy)_2](PF_6)_4$ (Figure 1a) was prepared by a literature procedure from the reaction of 2 equiv of $Ru(bpy)_2Cl_2$ and 1 equiv of tpphz.[24] The chloride salt of the complex (**2**) was precipitated from acetone by the addition of a saturated Bu_4NCl acetone solution, as previously reported for **1**.[10] Various purification steps were performed to ensure that **1** did not remain in the sample following the preparation of **2**. Although **2** was initially purified using a silica gel column, the sample was loaded onto a Sephadex G-15 column (2.5 cm diameter × 30 cm length) and was eluted with 0.1 M NaCl. Water was removed under vacuum, and the sample was redissolved in acetonitrile to remove the insoluble NaCl. The sample of **2** was then injected into a reverse-phase HPLC and was collected at times when complex **1** is known not to elute (Supporting Information). Electronic absorption, emission, excitation, and ^1H NMR spectroscopies were used to ascertain the purity of the sample. Owing to the significantly greater luminescence quantum yield of **1** as compared to that of **2**, the emission of the sample is affected greatly by purification even when the impurity is not observed in the ^1H NMR spectrum. The ^1H NMR spectrum of $[Ru(bpy)_2(tpphz)](PF_6)_2$ in CD_3CN is consistent with that previously reported for the complex,[24] and that of the corresponding chloride salt, **2**, is shown in the Supporting Information.

(26) Calvert, J. M.; Caspar, J. V.; Binstead, R. A.; Westmoreland, T. D.; Meyer, T. J. *J. Am. Chem. Soc.* **1982**, *104*, 6620.
(27) Demas, J. N.; Crosby, G. A. *J. Phys. Chem.* **1971**, *75*, 991.
(28) Rieger, P.H. *Electrochemistry*, 2nd ed.; Chapman & Hall: New York, 1994.
(29) Smith, S. R.; Neyhart, G. A.; Karlsbeck, W. A.; Thorp, H. H. *New J. Chem.* **1994**, *18*, 397.
(30) Carter, M. T.; Rodriguez, M.; Bard, A. J. *J. Am. Chem. Soc.* **1989**, *111*, 8901.
(31) Bradley, P. M.; Angeles-Boza, A. M.; Dunbar, K. R.; Turro, C. *Inorg. Chem.* **2004**, *43*, 2450.
(32) Nair, R. B.; Teng, E. S.; Kirkland, S. L.; Murphy, C. J. *Inorg. Chem.* **1998**, *37*, 139.
(33) Pyle, A. M.; Rehman, J. P.; Mehoyrer, R.; Kumar, C. V.; Turro, N. J.; Barton, J. K. *J. Am. Chem. Soc.* **1989**, *111*, 3051.
(34) Frisch, M. J.; Trucks, G. W.; Schlegel, H. B.; Scuseria, G. E.; Robb, M. A.; Cheeseman, J. R.; Montgomery, J. A., Jr.; Vreven, T.; Kudin, K. N.; Burant, J. C.; Millam, J. M.; Iyengar, S. S.; Tomasi, J.; Barone, V.; Mennucci, B.; Cossi, M.; Scalmani, G.; Rega, N.; Petersson, G. A.; Nakatsuji, H.; Hada, M.; Ehara, M.; Toyota, K.; Fukuda, R.; Hasegawa, J.; Ishida, M.; Nakajima, T.; Honda, Y.; Kitao, O.; Nakai, H.; Klene, M.; Li, X.; Knox, J. E.; Hratchian, H. P.; Cross, J. B.; Adamo, C.; Jaramillo, J.; Gomperts, R.; Stratmann, R. E.; Yazyev, O.; Austin, A. J.; Cammi, R.; Pomelli, C.; Ochterski, J. W.; Ayala, P. Y.; Morokuma, K.; Voth, G. A.; Salvador, P.; Dannenberg, J. J.; Zakrzewski, V. G.; Dapprich, S.; Daniels, A. D.; Strain, M. C.; Farkas, O.; Malick, D. K.; Rabuck, A. D.; Raghavachari, K.; Foresman, J. B.; Ortiz, J. V.; Cui, Q.; Baboul, A. G.; Clifford, S.; Cioslowski, J.; Stefanov, B. B.; Liu, G.; Liashenko, A.; Piskorz, P.; Komaromi, I.; Martin, R. L.; Fox, D. J.; Keith, T.; Al-Laham, M. A.; Peng, C. Y.; Nanayakkara, A.; Challacombe, M.; Gill, P. M. W.; Johnson, B.; Chen, W.; Wong, M. W.; Gonzalez, C.; Pople, J. A. *Gassian 03*, revision C.02; Gaussian, Inc.: Wallingford, CT, 2004.
(35) Becke, A. D. *Phys. Rev. A: Gen. Phys.* **1988**, *38*, 3098.
(36) Becke, A. D. *J. Chem. Phys.* **1993**, *98*, 5648.
(37) Lee, C.; Yang, W.; Parr, R. G. *Phys. Rev. B: Condens. Matter Mater. Phys.* **1988**, *37*, 785.
(38) Hehre, W. J.; Radom, L.; Schleyer, P. v. R.; Pople, J. A. *Ab Initio Molecular Orbital Theory;* Wiley & Sons: New York, 1986.
(39) Dolg, M.; Stoll, H.; Preuss, H. *Theor. Chim. Acta* **1993**, *85*, 441.
(40) Wedig, U.; Dolg, M.; Stoll, H. *Quantum Chemistry: The Challenge of Transition Metals and Coordination Chemistry;* D. Reidel: Dordrecht, The Netherlands, 1986.
(41) Fantacci, S.; De Angelis, F.; Selloni, A. *J. Am. Chem. Soc.* **2003**, *125*, 4381.
(42) De Angelis, F.; Fantacci, S.; Selloni, A. *Chem. Phys. Lett.* **2004**, *389*, 204.
(43) Cances, M. T.; Mennucci, B.; Tomasi, J. *J. Chem. Phys.* **1997**, *107*, 3032.
(44) Tomasi, J.; Persico, M. *Chem. Rev.* **1994**, *94*, 2027.
(45) Cossi, M.; Barone, V.; Mennucci, B.; Tomasi, J. *Chem. Phys. Lett.* **1998**, *286*, 253.
(46) Mennucci, B.; Tomasi, J. *J. Chem. Phys.* **1997**, *106*, 5151.
(47) Cossi, M.; Scalmani, G.; Rega, N.; Barone, V. *J. Chem. Phys.* **2002**, *117*, 43.
(48) Flükiger, P.; Lüthi, H. P.; Portmann, S.; Weber, J. *MOLEKEL 4.3;* Swiss National Supercomputing Centre CSCS: Manno, Switzerland, 2000; www.cscs.ch/molekel.

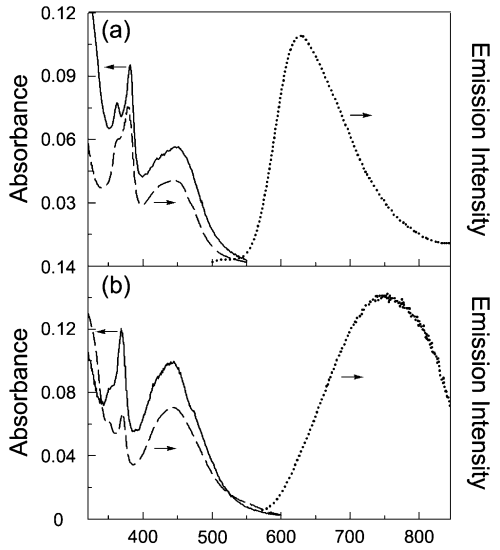

Figure 2. Absorption (—), excitation (– – –), and emission (· · ·, λ_{exc} = 430 nm) spectra of 3 μM (a) **1** and (b) **2** in CH_3CN. Excitation spectra were collected monitoring the emission at 634 nm for **1** and 749 nm for **2**.

Electronic Absorption and Emission in Solution. The electronic absorption spectra of **1** and **2** exhibit ligand-centered (LC) $^1\pi\pi^*$ transitions at ~285 nm from the bpy ligands and in the 350−400 nm region arising from the tpphz ligand, as well as Ru → bpy and Ru → tpphz ^{1}MLCT transitions in the visible region.[11,12] LC and MLCT absorptions are typical features of polypyridyl ruthenium complexes.[49,50] The lowest-energy ^{1}MLCT maxima of **1** are observed at 450 and 442 nm in CH_3CN and H_2O, respectively, while for **2** maxima at 442 and 444 nm are apparent in the same solvents, respectively. Although the absorption spectra of **1** and **2** are similar, there are two prominent differences apparent in Figure 2. The ratio of the intensities of the tpphz LC transitions (350−400 nm) to the MLCT transitions in CH_3CN is ~1:1 in **2**, while this ratio is 1.7:1 for **1** in the same solvent. This change in the ratio can be attributed to the 2:1 stoichiometry of ruthenium atoms to tpphz in **2**, which is 2-fold greater than the 1:1 Ru/tpphz ratio in **1**. Therefore, both complexes are expected to have the same number of tpphz transitions, with twice as many MLCT transitions in **2** compared to that in **1**. In addition, the absorption in the 500−600 nm region is greater in **2** than that in **1**. This absorption change is supported by TDDFT calculations, which show lower energy transitions in **2** compared to those calculated for **1** (Supporting Information).

Weak emission from the ^{3}MLCT excited state of **2** is observed in water with λ_{em} = 623 nm and $\Phi_{em} = 1.4 \times 10^{-4}$ (λ_{exc} = 400 nm), similar to that measured for **1** (λ_{em} = 634 nm, $\Phi_{em} = 1.7 \times 10^{-4}$).[10] A large red shift (λ_{em} = 749 nm) and 40-fold increase in intensity ($\Phi_{em} = 5.6 \times 10^{-3}$) is observed for the emission of **2** in acetonitrile relative to that in water (λ_{exc} = 400 nm). For comparison, complex **1** exhibits a maximum at 627 nm (Φ_{em} = 0.10) in CH_3CN, showing that the luminescence quantum yield of **2** in CH_3CN is 18-fold weaker than that of **1** in the same solvent.[10] An early report in 1996 cited the luminescence maxima of **1** and **2** in CH_3CN at 616 and 671 nm, respectively.[24] A later publication reported the emission maximum of **2** at 690 nm in CH_3CN,[25] and, more recently, emission maxima at 628 and 740 nm were published for **1** and **2**, respectively, in CH_3CN.[51] Because of the ~18-fold higher quantum yield of **1** as compared to that of **2** in CH_3CN, contamination of a sample of **2** with relatively small amounts of **1** (or other Ru(II) starting materials) will result in large deviations in the emission spectrum, the maximum of which will depend on the relative amount of impurity present. For example, addition of 6% **1** to a solution containing 13 μM **2** in CH_3CN results in a shift in the luminescence maximum from 749 to 670 nm. The excitation spectra in H_2O and CH_3CN of **1** and **2** are consistent with the respective absorption spectra in each solvent. Figure 2 shows the absorption, excitation, and emission spectra of both complexes in CH_3CN.

Table 1. Emission Maxima of **1** and **2** as a Function of Solvent Dielectric Constant (D_s)

		λ_{em}/nm	
solvent	D_s[a]	**1**	**2**
CH_2Cl_2	8.9	613	733
EtOH	24.3	623	733
MeOH	32.6	624	735
CH_3CN	36.2	627	749
DMSO	49	651	791
H_2O	78.4	634	623
DNA[b]		628	702[c]

[a] Values from ref 53. [b] ~3 μM complex, 100 μM DNA in 5 mM Tris, pH = 7.5, 50 mM NaCl. [c] Maximum for electrostatically bound complex.

The shift in the luminescence maximum from 634 nm in H_2O to 627 nm in CH_3CN for **1** is modest (ΔE = 176 cm^{-1}) and parallels observations for related $[Ru(bpy)_2(L)]^{2+}$ complexes, where L is a substituted dppz-type ligand, with values of ΔE that range from 133 to 264 cm^{-1}.[2,10] A similar comparison cannot be made for $[Ru(bpy)_2(dppz)]^{2+}$ since it is nonemissive in water. In contrast, the dependence of the emission maximum observed for **2** in the same solvents is significantly greater, with ΔE = 2700 cm^{-1}. Owing to this difference, the luminescent properties of **1** and **2** were investigated in several solvents with a range of dielectric constants, D_s. With the exception of H_2O, the emission maxima of both complexes shift to lower energy as the solvent polarity is increased (Table 1), indicative of a charge-transfer excited state.[52] In particular, the emission maximum of **1** shifts from 613 nm in CH_2Cl_2 to 651 nm in DMSO (ΔE = 952 cm^{-1}), as previously found for this complex.[51] For **2**, emission maxima at 733 and 791 nm are observed in CH_2Cl_2 and DMSO, respectively, corresponding to ΔE = 1000 cm^{-1}. This solvent dependence parallels that of **1** and is consistent with observations for $[Ru(bpy)_2(dppz)]^{2+}$ in the same solvents (ΔE = 1506 cm^{-1}). Similarly, the emission maximum of $[Ru(bpy)_3]^{2+}$ shifts from 606 nm in CH_2Cl_2 to 630 nm in DMF (D_s = 36.7), and to 634 nm in DMSO (ΔE = 729 cm^{-1}).[53−55] It should be pointed out, however, that the maxima recorded in the present work for complex **2** listed in Table 1 are red-shifted relative to those previously reported at 680 nm in CH_2Cl_2 and 780 nm in DMSO.[51]

(49) Juris, A.; Balzani, V; Barigelletti, F.; Campagna, S.; Belser, P.; Von Zelewsky, A. *Coord. Chem. Rev.* **1988**, *84*, 85.
(50) Watts, R. J. *J. Chem. Educ.* **1983**, *60*, 834.
(51) Chiorboli, C.; Bignozzi, C. A.; Scandola, F.; Ishow, E.; Gourdon, A.; Launay, J.-P. *Inorg. Chem.* **1999**, *38*, 2402.
(52) Chen, P.; Meyer, T. J. *Chem. Rev.* **1998**, *98*, 1439.
(53) Gordon, A. J.; Ford, R. A. *The Chemist Companion: A Handbook of Practical Data, Techniques, and References;* Wiley & Sons: New York, 1972.
(54) Caspar, J. V.; Meyer, T. J. *J. Am. Chem. Soc.* **1983**, *105*, 5583.
(55) Timpson, C. J.; Bignozzi, C. A.; Sullivan, B. P.; Kober, E. M.; Meyer, T. J. *J. Phys. Chem.* **1996**, *100*, 2915.

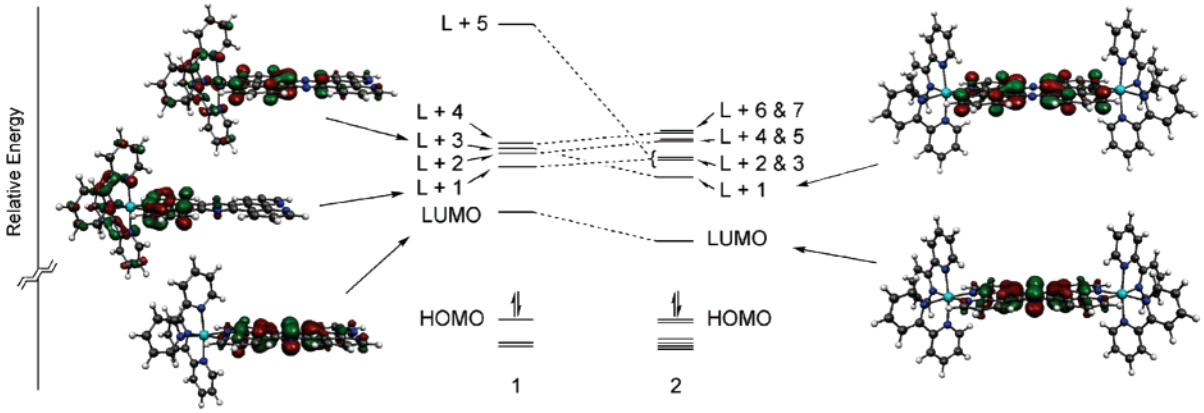

Figure 3. Molecular orbital diagrams comparing the relative energies of the frontier orbitals in **1** and **2**, where L + 1 represents LUMO + 1, and so forth. Selected orbitals are shown with an isovalue = 0.04.

Electronic Structure Calculations and Electrochemistry. DFT calculations were performed to aid in the interpretation of the differences in the excited-state behavior of **1** and **2**. In $[Ru(bpy)_2(dppz)]^{2+}$, it was previously shown that the lowest-energy ^{3}MLCT excited states correspond to charge transfer from Ru to the dppz ligand.[1,2] Charge transfer from the Ru(II) to MOs of the dppz with orbital contributions localized on the bpy portion of the ligand (closest to the metal) and those on the phenazine part (further from the metal) were proposed to correspond to emissive and nonemissive states, respectively.[20,21] A similar characterization can be made for the tpphz ligand in **1**, where ^{3}MLCT states with electron density on the phenazine (central) portion of the ligand and those on the distal bpy unit (further from metal) are expected to be nonemissive. In contrast, ^{3}MLCT states with electronic contribution from ancillary bpy ligands or the bpy portion of the tpphz ligand closest to the Ru center are likely to be emissive. In **2**, only ^{3}MLCT states with electronic contribution from the ancillary bpy ligands or the bpy portion of the tpphz ligand closest to the Ru center are expected to result in emissive excited states.

In both **1** and **2**, the DFT calculations show the presence of low-lying LC unoccupied π^* MOs that are expected to contribute in emissive and nonemissive MLCT states. For example, in **1** the electron density of the LUMO and LUMO + 3 orbitals are centered on the phenazine (central) portion of the tpphz ligand, such that an MLCT transition involving these orbitals would be expected to be nonemissive. Upon coordination of the *cis*-$[Ru(bpy)_2]^{2+}$ fragment to **1** to generate **2**, the energy of the LUMO + 3 in **1** decreases to become LUMO + 1 in **2** (Figure 3). The electron density of LUMO + 5 of **1** is centered on the distal bpy portion of the tpphz ligand, which would also result in a nonemissive MLCT state (Supporting Information). The energy of the LUMO + 5 in **1** decreases dramatically in **2**, corresponding to LUMO + 2 and LUMO + 3 in the latter. In addition, the MOs of **1** that possess emissive character, with electron density on the ligands near the Ru atom, such as LUMO + 1, increase in energy in **2** (Figure 3). In general, these changes reflect the presence of a greater fraction of lower-lying unoccupied MOs in **2** with nonemissive character compared to that in **1**. These calculations are consistent with the observed lower emission intensity of **2** relative to that of **1** in CH_3CN and with the lower emission energy of the former compared to the latter.

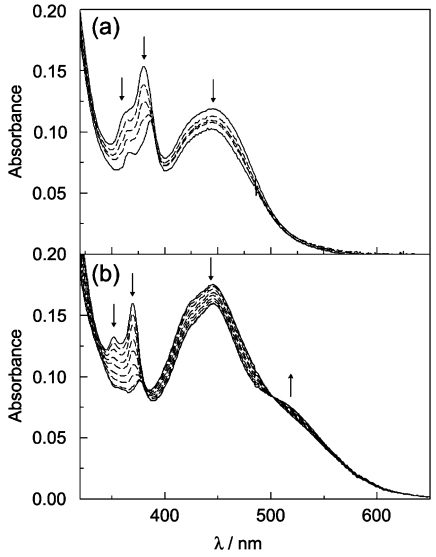

Figure 4. Changes to the electronic absorption spectra of 5 μM of (a) **1** and (b) **2** upon addition of up to 31 μM ct-DNA (50 mM NaCl, 5 mM Tris, pH = 7.5).

The results of the calculations are supported by the electrochemistry of **1** and **2**. The metal-centered oxidation potentials of both complexes are observed at +1.60 V vs NHE in CH_3CN (0.1 M $^tBu_4NPF_6$), a value typical for Ru(II) complexes with polypyridyl ligands.[49] For **2** in CH_3CN, the reduction of the tpphz ligand was observed at −0.53 V vs NHE, while that of **1** was found to occur at −0.73 V under similar experimental conditions.[10] The shift of +0.20 V in the reduction potential of **2** relative to that of **1** is consistent with the reduction of a tpphz ligand that is coordinated to transition metals at both bidentate coordination sites of the ligand.[10] The relative energy of the tpphz π^* LUMO of each complex obtained from the DFT calculations agrees with the ease of reduction of **2** compared to that of **1** (Figure 3). The calculated energy of the HOMO−LUMO gap of **2** is 0.18 eV smaller than that of **1** in CH_3CN, in agreement with the shift in the reduction potential.

Electronic Absorption and Luminescence Enhancement with DNA. The changes in the absorption spectra of **1** and **2** as a function of DNA concentration are illustrated in Figure 4. The tpphz $^1\pi\pi^*$ transition of **2** (5 μM) at 370 nm exhibits 44% hypochromicity and a 7 nm bathochromic shift in the presence of 31 μM ct-DNA (5 mM Tris, pH = 7.5, 50 mM NaCl). By

comparison, the hypochromicity reported for 5 μM of the intercalating complex **1** in the presence of 80 μM ct-DNA (5 mM Tris, pH = 7.5, 50 mM NaCl) was 38% at 380 nm, with a shift from 380 to 387 nm (Figure 4).[10] Further increase in the DNA concentration of each solution does not result in additional changes to the absorption spectrum of the complex. Hypochromicity in the ^{1}MLCT absorption bands of **1** and **2** is also observed upon addition of ct-DNA (Figure 4). In addition, in the presence of increasing concentrations of DNA, a low energy shoulder appears in the absorption spectrum of **2** at ~520 nm (Figure 4b), resulting in an isobestic point at 500 nm. The appearance of this low energy shoulder in the presence of DNA is not observed for **1** (Figure 4a).

The energy of the emission maxima of light-switch transition metal complexes is typically similar in CH_3CN and bound to DNA.[2] For example, $[Ru(bpy)_2(dppz)]^{2+}$ emits with a maximum at 618 nm both in CH_3CN and when intercalated between the DNA bases, but it is nonemissive at room temperature in water or buffer. Similarly, **1** emits at 627 nm in CH_3CN, and the luminescence maximum of the intercalated complex is observed at 628 nm and is weakly emissive in buffer (5 mM Tris, pH = 7.5, 50 mM NaCl), with maximum at 634 nm.[10] The data shows that there is little variation in the energy of the emission of $[Ru(bpy)_2(dppz)]^{2+}$ and **1** in CH_3CN, buffer, and bound to DNA. In contrast, a large shift in the emission maximum of **2** is observed upon addition of DNA from 623 to 702 nm (5 mM Tris, pH = 7.5, 50 mM NaCl), with maximum in CH_3CN at 749 nm. The excitation spectrum of 6 μM **2** in the presence of 100 μM DNA overlays well with the absorption spectrum of the complex bound to DNA (Supporting Information).

It should be pointed out that the emission maximum of **2** in the presence of DNA was recently reported by Rajput et al. to be 637 nm, which is significantly blue-shifted to that observed in the present work.[23] Furthermore, the maximum of **2** bound to DNA reported by Rajput et al. is blue-shifted with respect to that observed by the same authors in CH_3CN (λ_{em} = 671 nm).[23] A possible explanation for the difference in the results here and those reported by Rajput et al. is the presence of a small contamination of **1** in the sample in the latter. If this situation is the case, then some of the observed emission can be ascribed as arising from **1**, together with some luminescence from **2**, thus resulting in a maximum at an intermediate position between those of each complex. Unfortunately, the excitation spectrum of the complex in the presence of DNA was not reported by Rajput and co-workers.

The addition of 100 μM double-stranded poly(dA)·poly(dT) and poly(dAT)·poly(dAT) to 6 μM **2** resulted in 49- and 66-fold increase in emission intensity, respectively (5 mM Tris, pH = 7.5, 50 mM NaCl). In contrast, emission enhancements of 6 μM **2** by factors of only 8.6, 8.6, 13, and 5.3 were measured in the presence of 100 μM single-stranded poly(dA), poly(dC), poly(dT), and polystyrene sulfonate (PSS), respectively, in 5 mM Tris, pH = 7.5, 50 mM NaCl. These results indicate that protection of **2** from the aqueous environment by double-stranded DNA architectures is significantly better than that of single-stranded DNA and PSS.

DNA Binding. Binding constants, K_b, of **2** to ct-DNA were determined to be 5.1×10^7 M^{-1} (s = 2.7) and 4.5×10^7 M^{-1} (s = 2.2) from fits of the changes of the absorption and emission intensities of the complex, respectively, as a function of ct-DNA concentration (Supporting Information). In comparison, the changes in the emission intensity of **1** titrated with ct-DNA resulted in $K_b = 1.6 \times 10^6$ M^{-1} (s = 2.4). The values of K_b calculated from equilibrium dialysis of **1** and **2** with ct-DNA were 3.5×10^5 and 1.9×10^5 M^{-1}, respectively.[10] As reported previously for **1**,[10] fits of the absorption and emission changes of the complexes as a function of ct-DNA lead to significantly greater K_b values than equilibrium dialysis. This difference is attributed to absorption and emission changes due to aggregation of the probe molecules in solution or on the surface of the polyanion. Since the optical changes of the probe in the presence of DNA are not likely to be a result of a 1:1 complex/base interaction, fits that assume such a binding model may not be useful for obtaining accurate DNA binding constants for complexes that exhibit aggregation in water and/or on the DNA surface. Similar results were also reported for other cationic metal complexes with extended hydrophobic ligands.[56]

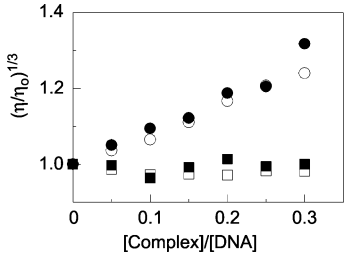

Figure 5. Relative viscosity measurements of 1 mM sonicated herring sperm DNA upon addition of increasing concentrations of ethidium bromide (●), $[Ru(bpy)_2(dppz)]^{2+}$ (○), Hoecht 33258 (■), and **2** (□).

Several techniques were employed to elucidate the DNA binding mode of **2** to ds-DNA. The determination of the shift in the DNA melting temperature in the presence of **2** was not possible owing to the strong absorption of the complex at 260 nm, such that absorption changes at this wavelength do not simply reflect the denaturation of the double helix. Relative viscosity measurements have been shown to be a reliable technique to determine intercalation by probe molecules.[57] Addition of increasing concentrations of **2** to 1 mM herring sperm DNA (5 mM Tris, pH = 7.5, 50 mM NaCl) does not result in an increase in the relative viscosity of the solution (Figure 5), showing that the complex is not an intercalator. Similar results were observed for the minor groove binder Hoechst 33258 (Figure 5), as well as $[Ru(bpy)_3]^{2+}$, which do not intercalate between the DNA bases.[58] In contrast, an increase in relative viscosity is observed for DNA solutions in the presence of the intercalators ethidium bromide (EtBr) and $[Ru(bpy)_2(dppz)]^{2+}$ (Figure 5), as well as **1**.[10] It should be noted that Rajput et al. reported an increase in the relative viscosity by a factor of 1.03 at [DNA bp]/[complex] = 0.2; however, this value is significantly lower than that measured for **1** and EtBr at similar concentrations (~1.2, Figure 5). The small increase in viscosity for **2** noted in this work can be explained by the presence of a small amount of the intercalating complex **1** in solution as an impurity.

The ionic strength dependence of the DNA binding constant can also be used to distinguish between intercalation and electrostatic binding. For **1**, the DNA binding constants were

(56) Angeles-Boza, A. M.; Bradley, P. M.; Fu, P. K.-L.; Wicket, S. E.; Bacsa, J.; Dunbar, K. R.; Turro, C. *Inorg. Chem.* **2004**, *43*, 8510.
(57) Suh, D.; Oh, Y.-K.; Chaires, J. B. *Process Biochem.* **2001**, *37*, 521.
(58) Comings, D. C. *Chromosoma* **1975**, *52*, 229.

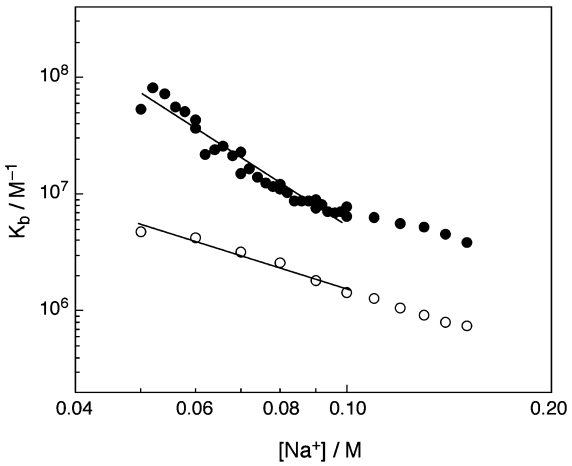

Figure 6. Log plot of K_b vs [Na^+] for **1** (○) and **2** (●).

measured to be 1.6×10^6 M^{-1} ($s = 2.4$) and 1.7×10^6 M^{-1} ($s = 1.8$) in 50 mM and 1 M NaCl (5 mM Tris, pH = 7.5), respectively (Supporting Information). The independence of K_b on salt concentration for **1** is consistent with intercalation of the complex. In contrast, K_b values of 4.5×10^7 M^{-1} ($s = 2.2$) and 1.2×10^6 M^{-1} ($s = 3.3$) were measured for **2** in 50 mM and 1 M NaCl (5 mM Tris, pH = 7.5), respectively (Supporting Information). A similar salt dependence of the DNA binding was also reported by Rajput et al. for **2**. The ionic strength dependence of binding of **2**, with an overall charge of +4, to DNA is consistent with binding driven by significant electrostatic contribution, not intercalation.

Reverse salt titrations of **1** and **2** bound to DNA were performed, and the results are shown in Figure 6. The reverse salt titration was performed with a 2 mL sample containing 3 μM **2** and 11 μM ct-DNA (50 mM NaCl, 5 mM tris, pH = 7.5), such that ~65% of **2** was bound before the titration. A 5 M NaCl solution was titrated into the sample in 2 μL aliquots, and the decrease in luminescence was monitored.[59,60] A similar experiment was performed for **1** using 10 μM complex and 53 μM DNA resulting in ~90% binding before the titration. The binding constant at each titration point was then calculated, and a plot of log[K_b] vs log[Na^+] was constructed (Figure 6). From polyelectrolyte theory,[61] the slope of this graph provides an estimate of $SK = \delta \log[K_b]/\delta \log[Na^+] = -Z\psi$, where Z is the charge of the metal complex and ψ is 0.88 for ds-DNA.[59,62,63] Figure 6 shows the decrease of K_b of **2** as the concentration of Na^+ is increased. As expected, the plot becomes nonlinear at ionic strengths greater than 0.1 M.[59,61] For **2** at [Na^+] < 0.1 M, SK = −3.5450, resulting in $Z = +4.0 \pm 0.3$, consistent with the +4 charge of **2**. For **1** (Figure 6), SK = −1.6337 and $Z = +1.9 \pm 0.1$, consistent with the +2 charge of **1** and with results previously reported for Δ- and Λ-$[Ru(bpy)_2(dppz)]^{2+}$.[59]

Thermodynamic parameters can also be calculated from the DNA binding constants for each complex, resulting in the observed Gibbs free energy of binding, ΔG_{obs}. The polyelectrolyte and nonelectrostatic components of ΔG_{obs} can be separated, ΔG_{pe} and ΔG_t, respectively, as previously reported.[59,64] For complexes **1** and **2**, these parameters are listed in Table 2, along with those published for related complexes.[59] It is evident from Table 2 that complex **1** exhibits a greater contribution to ΔG_{obs} from its nonelectrostatic binding (66%) than from Coulombic interactions (34%) with DNA, as expected for an intercalator. The magnitudes of ΔG_{obs}, ΔG_{pe}, and ΔG_t calculated here for **1** are very similar to those previously reported for $[Ru(phen)_2(dppz)]^{2+}$, a related intercalator with similar molecular structure (Table 2), with 37% contribution to ΔG_{pe} for the Δ-isomer.[59] For comparison, the monovalent intercalator ethidium bromide exhibits significantly lower contribution from its electrostatic component (23%). In contrast, complex **2** exhibits a significantly greater contribution to the Gibbs free energy from the polyelectrolyte component (61%) than from nonelectrostatic interactions (39%). The results for **2** are qualitatively similar to those of $[Ru(phen)_3]^{2+}$, which interacts with DNA through electrostatic binding and hydrophobic interactions in the major groove, resulting in greater relative contribution to ΔG_{obs} from ΔG_{pe} (44%) than ΔG_t (56%) than for the intercalators. Together these results are consistent with the intercalation of **1** and the electrostatic surface binding of **2**.

Table 2. Comparison of ΔG Values (kcal mol^{-1}) for Various Complexes Binding to DNA

complex	$-\Delta G_{obs}$	$-\Delta G_{pe}$	$-\Delta G_t$
1	8.5	2.9	5.6
2	10.4	6.3	4.1
Δ-$[Ru(phen)_2(dppz)]^{2+}$ [a]	8.9	3.3	5.6
Λ-$[Ru(phen)_2(dppz)]^{2+}$ [a]	8.5	3.7	4.8
Δ-$[Ru(phen)_3]^{2+}$ [a]	5.4	2.4	3.1
Λ-$[Ru(phen)_3]^{2+}$ [a]	5.5	2.2	3.4
ethidium bromide	8.3	1.9	5.8

[a] From ref 59.

Photogenerated Threaded Intercalator. Although the relative viscosity data show that **2** does not intercalate between the DNA bases, it is important to ensure that the emission enhancement of the complex upon addition of DNA discussed earlier did not arise from threading intercalation of the complex. Bimetallic threaded intercalators published by Nordén require long incubation times for this mode of binding to be attained (2 weeks at room temperature under typical ionic strength conditions);[65] alternatively, high salt concentrations (100−300 mM NaCl) and higher temperature (45 °C) have also been shown to induce the threading intercalation in shorter times (1 h to 1 day). Since the emission experiments reported in this work were conducted immediately after mixing the complex with the DNA at room temperature in 50 mM NaCl (5 mM Tris, pH = 7.5), threading intercalation is not expected for **2** under these conditions. In addition, several unsuccessful attempts were made to thread **2** into ds-DNA. For example, ct-DNA incubated with the complex over a period of five days at room temperature in 50 mM NaCl, 5 mM Tris, pH = 7.5 did not result in any changes to the absorption or emission properties of the sample. Attempts to thread **2** into ds-DNA by melting a 18-mer oligonucleotide duplex and ct-DNA at 90 °C for 5 min in the presence of the complex followed by slow cooling were

(59) Haq, I.; Lincoln, P.; Suh, D.; Norden, B.; Chowdhry, B. Z.; Chaires, J. B. *J. Am. Chem. Soc.* **1995**, *117*, 4788.
(60) Lohman, T. M.; Mascotti, D. P. *Methods Enzymol.* **1992**, *212*, 424.
(61) Record, M. T.; Anderson, C. F.; Lohman, T. M. *Q. Rev. Biophys.* **1978**, *86*, 469.
(62) Mudasir, Wijaya, K.; Wahyuni, E. T.; Yoshioka, N.; Inoue, H. *Biophys. Chem.* **2006**, *121*, 44.
(63) Liu, F.; Wang, K.; Bai, G.; Zhang, Y.; Gao, L. *Inorg. Chem.* **2004**, *43*, 1799.
(64) Hopkins, H. P.; Wilson, W. D. *Biopolymers* **1987**, *26*, 1347.
(65) Wilhelmsson, L. M.; Westerlund, F.; Lincoln, P.; Nordén, B. *J. Am. Chem. Soc.* **2001**, *123*, 3630.

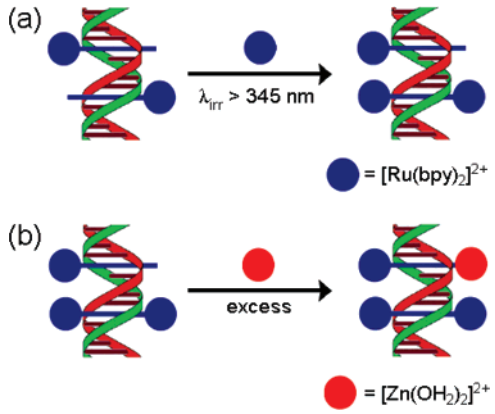

Figure 7. Schematic representation of (a) the photogeneration of threaded **2** from the photolysis of $[Ru(bpy)_2(CH_3CN)_2]^{2+}$ in the presence of DNA-intercalated **1** and (b) addition of excess $ZnCl_2$ to quench the emission of unreacted **1**.

also unsuccessful (50 mM NaCl, 5 mM Tris, pH = 7.5). Although the generation of the threaded intercalator starting with **2** was not possible under our experimental conditions, we have been able to attain it photochemically in a stepwise fashion as described in the next paragraph.

Complex **2** was generated from the reaction of **1** with photochemically generated *cis*-$[Ru(bpy)_2]^{2+}$ fragment, and its formation was followed by the increase in its luminescence in CH_3CN. A 2 mL CH_3CN solution containing 10 μM **1** (λ_{em} = 628 nm) and 100 μM *cis*-$[Ru(bpy)_2(CH_3CN)_2]^{2+}$ (no luminescence at 298 K) was irradiated for 15 min (λ_{irr} > 395 nm), which resulted in a 2-fold decrease of the emission of **1**. Owing to the presence of unreacted **1**, with 18-fold greater emission quantum yield than that of **2** in CH_3CN, the emission maximum remained at 630 nm. Since binding of Zn^{2+} to the distal nitrogen atoms of the tpphz ligand of **1** has been previously shown to quench all the emission from the complex, 100 μM $Zn(BF_4)_2$ was added to the irradiated sample. Upon quenching of the contribution to the luminescence of **1** with Zn^{2+}, a maximum at 749 nm was observed, where authentic **2** emits in CH_3CN. This experiment clearly shows that the photolysis of $[Ru(bpy)_2(CH_3CN)_2]^{2+}$ with **1** results in the formation of **2**. HPLC separation of the photolysis mixture shows the formation of **2** (Supporting Information, Figure S7).

The photolysis of $[Ru(bpy)_2(CH_3CN)_2]^{2+}$ with **1** was also conducted in the presence of DNA. Complex **1** (10 μM) was intercalated in 200 μM ct-DNA (50 mM NaCl, 5 mM Tris, pH = 7.5) as previously reported,[10] which exhibits an emission with maximum at 627 nm. $[Ru(bpy)_2(CH_3CN)_2]^{2+}$ (100 μM) was added to this solution, and the sample was irradiated for 15 min with λ_{irr} > 395 nm (Φ_{aq} = 0.44, λ_{irr} = 436 nm),[66] thus resulting in the formation of **2** intercalated in DNA in a threading fashion (Figure 7a). After the photolysis, the emission intensity decreased by a factor of 2.6, and the luminescence of unreacted **1** was quenched through the addition of 100 μM $ZnCl_2$ (Figure 7b).[10] The addition of $ZnCl_2$ does not quench the emission of **2**, and therefore, the remaining emission with maximum at 685 nm is assigned as arising from intercalated **2**. The blue shift in the luminescence of photogenerated **2** intercalated in ct-DNA, compared to that of the electrostatically bound complex (702 nm), can be attributed to the better protection from the aqueous environment in the former.

It should be pointed out that, at room temperature, samples of 100 μM $[Ru(bpy)_2(CH_3CN)_2]^{2+}$ alone (50 mM NaCl, 5 mM Tris, pH = 7.5) and in the presence of 200 μM ct-DNA (50 mM NaCl, 5 mM Tris, pH = 7.5) are nonemissive. No luminescence was detected following the photolysis of 100 μM $[Ru(bpy)_2(CH_3CN)_2]^{2+}$ (λ_{irr} > 395 nm, 15 min) alone and with 200 μM ct-DNA (50 mM NaCl, 5 mM Tris, pH = 7.5), showing that the emission does not arise from this complex or its photoproducts.

Conclusions

Complexes **1** and **2** exhibit absorption and emission spectra that are typical of related Ru(II) complexes. The maximum of the ^{3}MLCT luminescence of each complex is dependent on the polarity of the solvent, a fact that is consistent with a charge-transfer excited state. Electronic structure calculations on **1** and **2** show the changes in the character of the low-lying ligand-centered π^* orbitals on the tpphz ligand expected to participate in emissive and nonemissive MLCT transitions, thus explaining the difference in emission quantum yields of the complexes.

Complex **1** binds to DNA via intercalation of the tpphz ligand; conversely, various techniques, including relative viscosity measurements, reveal that **2** does not intercalate. The emission intensity of both complexes, however, increases upon the addition of DNA. Complex **2** intercalated between the DNA bases in a threaded fashion was generated photochemically from intercalated **1**. The emission maximum of threaded **2** is different from that of the complex that is electrostatically bound to DNA.

To our knowledge, the present work is the first example of a nonintercalating light-switch metal complex with double-stranded DNA, thus showing that light-switch behavior cannot be used exclusively as confirmation of intercalation.

Acknowledgment. C.T. thanks the National Science Foundation (CHE 0503666) and the Ohio Supercomputing Center. K.R.D. thanks the State of Texas for an ARP grant (010366-0277-1999) and the Welch Foundation (A1449) for financial support.

Supporting Information Available: Figures S1−S7, eq S1, and Table S1. This material is available free of charge via the Internet at http://pubs.acs.org.

JA071001V

(66) Pinnick, D. V.; Durham, B. *Inorg. Chem.* **1984**, *23*, 1440.